

Performance of Zernike polynomials in reconstructing raw-elevation data captured by Pentacam HR, Medmont E300 and Eye Surface Profiler

Yueying Wei^{1,2}, Bernardo T Lopes^{3,4}, Ashkan Eliasy³, Richard Wu⁵,
Arwa Fathy⁶, Ahmed Elsheikh^{3,7-8}, Ahmed Abass^{2,9*}

¹ Department of Chemical Engineering and Applied Chemistry, University of Toronto, Toronto, Ontario, Canada

² Department of Mechanical, Materials and Aerospace Engineering, School of Engineering, University of Liverpool, Liverpool, UK

³ Department of Civil Engineering and Industrial Design, School of Engineering, University of Liverpool, Liverpool, UK

⁴ Department of Ophthalmology, Federal University of Sao Paulo, Sao Paulo, Brazil

⁵ Brighten Optix Corporation, Shilin District, Taipei City, Taiwan

⁶ Wirral Grammar School for Girls, Bebington, Wirral Peninsula, UK

⁷ School of Biological Science and Biomedical Engineering, Beihang University, Beijing, China

⁸ National Institute for Health Research (NIHR) Biomedical Research Centre at Moorfields Eye Hospital NHS Foundation Trust and UCL Institute of Ophthalmology, London, UK

⁹ Department of Production Engineering and Mechanical Design, Faculty of Engineering, Port Said University, Egypt

* **Author for correspondence:** Dr Ahmed Abass

School of Engineering, University of Liverpool, Liverpool, L69 3GH, UK.

A.Abass@liverpool.ac.uk

Keywords: Corneal tomography, Pentacam, Zernike polynomials, Signal processing, Curve fitting

Number of words: 6050

34 **Abstract**

35 **Purpose:** To investigate the capability of Zernike polynomials fitting to reconstruct corneal
36 surfaces as measured by Pentacam HR tomographer, Medmont E300 Placido-disc and Eye
37 Surface Profiler (ESP).

38 **Methods:** The study utilised a collection of clinical data of 527 participants. Pentacam HR raw
39 elevation data of 660 eyes (430 healthy and 230 keratoconic) were fitted to Zernike
40 polynomials of order 2 to 20. Same analyses were carried out on 158 eyes scanned by
41 Medmont E300 Placido-disc and 236 eyes were scanned by ESP for comparison purposes.
42 The Zernike fitting was carried out using a random 80% of each individual eye
43 surface's data up to a corneal radius of 5 mm and the root means squared fitting error
44 (RMS) was calculated for the unused 20% portion of the surface data. The process was carried
45 out for the anterior and posterior surfaces of the corneal measurements of the Pentacam and
46 the anterior surfaces only with the ESP and the Medmont E300 measurements.

47 **Results:** Statistical significances in reduction of RMS were noticed up to order 14 among
48 healthy participants ($p < 0.0001$ for right eyes, $p = 0.0051$ for left eyes) and up to order 12
49 ($p < 0.0001$ for right eyes, $p = 0.0002$ for left eyes) in anterior surfaces measured by the
50 Pentacam. Among keratoconic eyes, statistical significance was noticed up to order 12 in both
51 eyes ($p < 0.0001$ for right eyes, $p = 0.0003$ for left eyes). The Pentacam posterior corneal data,
52 both right and left, healthy and keratotic eyes recorded significance ($p < 0.0001$) in reduction of
53 RMS up to order 10 with same RMS values of 0.0003 mm with zero standard deviation. RMS
54 of fitting Zernike polynomials to Medmont data up to order 20 showed a consistent reduction
55 in RMS with the increase of the fitting order with no rise at high fitting orders. Minimum
56 $\text{RMS} = 0.0047 \pm 0.0021$ mm, 0.0046 ± 0.0019 mm for right and left eyes respectively were
57 recorded at order 20 and were more than 15 times the minimum RMS of the Pentacam. RMS
58 of fitting Zernike polynomials to ESP data also showed a consistent reduction in RMS with the
59 increase of the fitting order with no sign of any rise at high fitting orders. Similar to the
60 Medmont, minimum RMS of 0.0005 ± 0.0003 mm, 0.0006 ± 0.0003 mm was recorded at order

61 20 for right and left eyes respectively and was 2 times the minimum RMS of the Pentacam for
62 right eyes and 1.7 times the minimum RMS of the Pentacam for left eyes.

63 **Conclusions:** Orders 12 and 10 Zernike polynomials almost perfectly matched the raw-
64 elevation data collected from Pentacam for anterior and posterior surfaces, respectively for
65 either healthy or keratoconic corneas. The Zernike fitting could not perfectly match the data
66 collected from Medmont E300 and ESP.

67

68

69

70

71

72

73

74

75

76

77

78

79

80

81

82 Introduction

83 Although several instruments reconstruct anterior eye features in the market with good
84 repetitions in terms of accuracy and repeatability, the common recommendation from the
85 literature is not to use measured values interchangeably among these instruments ^{1, 2}.
86 Because these instruments use different approaches and different mathematical algorithms to
87 reproduce the corneal topography and tomography, there is no surprise that their final
88 readings are not always comparable ^{3, 4}. Therefore, understanding the theory and the data
89 handling in each device, hence choosing a suitable mathematical algorithm to reconstruct the
90 measured surfaces would reduce the differences among devices when used to evaluate the
91 same phenomenon. The Pentacam captures sets of cross-sectional images using the
92 Scheimpflug camera, while the Medmont Placido-disc analyses the reflected image of
93 concentric rings, and the Eye Surface Profiler (ESP) captures sinusoidal grating projected
94 images using a charge-coupled device (CCD) camera. Due to these differences, the measured
95 object does not directly represent corneal topography or tomography. Therefore, post-
96 measurement digital signal processing (DSP) procedures are required where the measured
97 data sets are treated in certain ways to represent the anterior eye topography or tomography.
98 Hence refractive power maps and other outputs that eye clinicians use for their diagnosis of
99 eye disorders are influenced by these analyses. Among many other aspects, DSP involves
100 enhancement, representation, reconstruction and, in some cases, interpretation of signals.

101

102 Typically, to protect their intellectual property (IP) ⁵, manufacturers do not always provide full
103 detailed information about the way their instruments process the measured data, therefore,
104 this part of the post-measurement processing is usually unseen by the users and hence, its
105 effect cannot be evaluated directly with conventional approaches ⁶. In addition, software-
106 related concerns in medical devices are not rare and could influence health care ⁷. Therefore,
107 the current study uses a reverse engineering approach to investigate the post-measurement
108 DSP algorithm in three different instruments and evaluate its effect on the instruments'

109 measurements. The study investigates the prospect of the use of Zernike polynomial to fit the
110 raw-elevation data and how this possibility could be accounted for or even used by engineers
111 who are using Zernike polynomial to fit Pentacam raw elevation data for the purposes of
112 modelling corneal surfaces or to carry out wavefront analyses.

113

114 **Materials and Methods**

115 **Participants**

116 In this record review analysis, no participant had been recruited specially for this study,
117 therefore fully anonymised secondary data was used. The study utilised a collection of clinical
118 data that has been used in various previous studies⁸⁻¹⁸ where only valid data, in terms of
119 quality, were selected to be processed. Recorded data for individuals who were suffering from
120 ocular diseases or have a history of trauma or ocular surgery, including Asian upper
121 blepharoplasty, were excluded. Additionally, those with intraocular pressure (IOP) higher than
122 21 mmHg as measured by the Goldmann Applanation Tonometer, soft contact lens wear until
123 less than two weeks before measurement, or rigid gas-permeable (RGP) contact lens wear
124 until less than four weeks before measurements were excluded.

125 In order to avoid bias, right and left eyes were always treated independently from each other,
126 and no merging data technique was applied in this work. According to the University of
127 Liverpool's Policy on Research Ethics, ethical approval was unnecessary for secondary
128 analysis of fully anonymised data. Nevertheless, the study followed the tenets of the Helsinki
129 Declaration.

130

131 **Pentacam HR data**

132 The study used a recorded data of both eyes of 330 healthy participants aged 35.6 ± 15.8 years
133 and 230 Keratoconic participants aged 31.6 ± 10.8 years. Participants were selected from
134 referrals to Hospital de Olhos Santa Luzia, Maceio, Alagoas, Brazil. Clinical tomography data

135 has been collected from both eyes of participants using the Pentacam HR (OCULUS
136 Optikgeräte GmbH, Wetzlar, Germany). Pentacam HR raw elevation data for the anterior
137 surface were exported in comma-separated values (CSV) format and analysed using custom-
138 built MATLAB codes (MathWorks, Natick, USA). Data was extracted over a mesh grid covering
139 -7 to 7 mm in 141 steps in both nasal-temporal and superior-inferior directions with missing
140 elevation values around corners and edges set to NaN which stands for “Not a Number”. The
141 effect of missing elevation values was automatically avoided arithmetically and
142 logically during the analyses. This is because any arithmetic operation in MATLAB that
143 involves a NaN produces a NaN as well. Furthermore, MATLAB logical operations (true-
144 false) involving NaNs always return as false.

145

146

147 **Medmont E300 data**

148 Medmont E300 Placido-disc elevation data for the corneal anterior surface were exported in
149 Microsoft Excel spreadsheet (XLSX) format and analysed using custom-built MATLAB codes.
150 Data was extracted over a mesh grid covering -6 to 6 mm in 50 steps in both nasal-temporal
151 and superior-inferior directions with missing elevation values around the edges set to a big
152 negative value of -5×10^{20} .

153 Both right and left eye anonymised topography data were extracted from the recorded data of
154 79 Caucasians (158 eyes); 41 females and 38 males aged 43.3 ± 11.5 . The eye surface scan
155 process was carried out using the Medmont E300 corneal topographer (Medmont
156 International, Nunawading, Australia).

157

158

159 **ESP data**

160 Both right and left eye anonymised topography data were extracted from the recorded data of
161 both eyes of 125 Taiwanese Asian and 118 Caucasian subjects aged 22 to 67 years
162 (38.5 ± 7.6). Groups were properly gender-balanced (Asians: 66 females and 59 males;
163 Caucasians: 63 females and 55 males). The eye surface scan process was carried out using
164 ESP, a non-contact corneo-scleral topographer, Eaglet Eye BV, AP Houten, The
165 Netherlands).

166 The data was exported from the ESP software in MATLAB binary data container format (*.mat)
167 where the characteristics of eyes, as measured by the ESP system, were extracted and
168 processed. The eye surface data was processed by custom-built MATLAB codes independent
169 from the built-in ESP software. Data was extracted over a mesh grid covering -10 to 10 mm in
170 700 steps in the nasal-temporal direction, and -8 to 8 mm in 800 steps in the superior-inferior
171 direction with missing elevation values around the edges set to NaN.

172

173 **Corneal surfaces fitting**

174 Three-dimensional curve fitting is a process that aims to reconstruct a surface through a
175 parametric mathematical expression or nonparametric method that best suits a cloud of data
176 points. In the current study, Zernike polynomials were used as parametric mathematical
177 expressions that are capable of reconstructing corneal surfaces. As each one of the three
178 instruments used in this study is able to cover the cornea to different diameters, a maximum
179 radius of 5 mm was used in the fitting exercise for all instruments, Figure 1. Any surface data
180 beyond this maximum radius were set to NaN, hence disregarded in these analyses.
181 Therefore, the surface grid is centred around the corneal apex, then the radius of each point
182 in R_g the grid is calculated in Eq.1 as

$$r = \sqrt{X_g^2 + Y_g^2} \quad \& \quad Z_g(r > 5) = NaN \quad (\text{Eq.1})$$

183 where X_g and Y_g represent the grid points in the nasal-temporal and superior-inferior
 184 directions, respectively and Z_g is the corneal raw elevation.

185 Once the data within the 5 mm radius was identified, the Zernike polynomial fit sequence was
 186 carried out with orders 1 to 20 using the minimum least squared error method and the root-
 187 mean-square (RMS) error values were recorded for each fit. At this point, a normalised form
 188 of the radius r was calculated in Eq. 2 as

$$r_n = \frac{r}{r_{max}}, \text{ where } r_{max} = 5mm \quad (\text{Eq. 2})$$

189

190 Zernike polynomials used the polar coordinates (r_n, θ) and the relevant raw elevation data
 191 obtained for each cornea to express the radial distance ρ as presented in Eq. 3.

$$\rho = \sum_{n=0}^{\text{order}} \sum_{m=-n:2:n} Z_n^m(r, \theta) C_n^m(\theta) \quad (\text{Eq. 3})$$

192 Where Zernike term is represented by Eq. 4 as

$$Z_n^m(r, \theta) = \begin{cases} R_n^{|m|} \cos(m\theta) & m > 0 \\ R_n^{|m|} \sin(m\theta) & m < 0 \\ R_n^0 & m = 0 \end{cases} \quad (\text{Eq. 4})$$

193 with the radial polynomial $R_n^{|m|}$ defined in Eq.5 as

$$R_n^{|m|} = \sum_{i=0}^{\frac{n-|m|}{2}} \frac{(-1)^i (n-i)! r^{n-2i}}{i! ((n+|m|)/2 - i)! ((n-|m|)/2)!}, \quad (0 \leq r \leq 1) \quad (\text{Eq. 5})$$

194 Where (r, θ) are the polar coordinates of X_g and Y_g , n is the radial order of the polynomial,
 195 and m is an azimuthal integer index that varies from $-n$ to n for even $(m-n)$ and equals 0 for
 196 odd $(n-m)$. The fitting root mean square (RMS) error was calculated twice for every fit during
 197 the fitting process, firstly by using the whole surface for fitting and validation, then secondly by
 198 randomly selecting 80% of the data points for fitting and the other 20% to calculate the fitting
 199 RMS error by Eq.6 as

$$RMS = \sqrt{\frac{\sum_{i=1}^k (Z_{i\ fit} - Z_{i\ surf})^2}{k}} \quad (\text{Eq. 6})$$

200 where Z_{fit} is the Zernike fitted surface height and Z_{surf} is the measured raw elevation surface
201 height and k is the number of non-missing data points. In this study, the RMS error represents
202 the squared root of the averaged squared variations between fitted surface height points Z_{fit}
203 and clinically observed surface height points Z_{surf} . The process was carried out for the
204 anterior and posterior surfaces of the corneal measurements of the Pentacam and the anterior
205 surfaces only with the ESP and the Medmont E300 Placido-disc measurements as both of
206 them measure the corneal anterior surface only.

207

208 **Statistical analysis**

209 Statistical analysis was performed using MATLAB Statistics and Machine Learning Toolbox
210 (MathWorks, Natick, USA). The null hypothesis probability (p) at 95% confidence level was
211 calculated to compare each set of RMS errors when a corneal surface was fitted to Zernike
212 polynomial with a certain order with the set of RMS errors when the same corneal surface was
213 fitted to Zernike polynomial with one order less. Initially, the one-sample Kolmogorov-Smirnov
214 test was used to make sure that each set of RMS errors follows a normal distribution, then the
215 two-sample t-test was used to investigate the significance between pairs of data sets to check
216 whether the results represent independent records. The probability p is an element of the
217 period $[0,1]$ where values of p higher than 0.05 indicate the validity of the null hypothesis and
218 values less than or equal to 0.05 indicate the invalidity of the null hypothesis, hence statistical
219 significance ¹⁹.

220

221 **Results**

222 The results showed that the Pentacam anterior surface Zernike polynomial fitting RMS
223 decreased with the increase of the fitting order, Table 1, however, the small values of the RMS

224 error from order 10 (RMS=0.0004±0.0001 mm for right eyes, RMS=0.0005±0.0002 mm for
225 left eyes) to 15 (RMS=0.0003±0.0001 mm for right eyes, RMS=0.0004±0.0015 mm for left
226 eyes) were notable in healthy subjects. The same phenomenon was noticed in keratoconic
227 patients between order 10 (RMS= 0.0005±0.0002 mm for right eyes, RMS=0.0005±0.0002
228 mm for left eyes) and order 15 (RMS=0.0003±0.0002 mm for right eyes, RMS=0.0004±0.0003
229 mm for left eyes). From fitting order 16, RMS values started to rise exponentially to record
230 0.1221±0.8218 mm, 0.0837±0.7085 mm, 0.1419±1.6770 mm, 0.2564±0.4612 mm for healthy
231 right and left eyes and keratoconic right and left eyes, respectively, Figure 2.

232 To evaluate the quality of fitting of each order against the previous order, the two samples t-
233 test was used to compare the RMS of each order with the previous order, Figure 3. When the
234 difference in RMS values at each order n compared to the previous order n-1, statistical
235 significances were noticed up to order 14 among healthy participants (p<0.0001 for right eyes,
236 p=0.0051 for left eyes) and up to order 12 (p<0.0001 for right eyes, p=0.0002 for left eyes).
237 Among keratoconic eyes, statistical significance was noticed up to order 12 in both eyes
238 (p<0.0001 for right eyes, p= 0.0003 for left eyes).

239 Remarkably, when the corneal posterior surface was investigated in the Pentacam data, both
240 eyes right and left eyes of healthy and keratotic participants recorded significance (p<0.0001)
241 in fitting RMS up to order 10 with the same RMS values of 0.0003 mm and zero standard
242 deviation for all right, left, healthy and keratotic eyes, Table 2.

243 Unlike the Pentacam tomography fitting outcome, RMS of fitting Zernike polynomials to
244 Medmont data up to order 20 showed a consistent reduction in RMS with the increase of the
245 fitting order with no rise at high fitting orders, Figure 4. Minimum RMS=0.0047±0.0021 mm,
246 0.0046±0.0019 mm for right and left eyes respectively were recorded at order 20 and were
247 more than 15 times the minimum RMS of the Pentacam, Table 3.

248 Like the Medmont Placido disc, and unlike the Pentacam tomography fitting outcome, RMS of
249 fitting Zernike polynomials to ESP data up to order 20 also showed a consistent reduction in

250 RMS with the increase of the fitting order with no sign of any rise at high fitting orders, Figure
251 5. Similar to the Medmont, minimum RMS of 0.0005 ± 0.0003 mm, 0.0006 ± 0.0003 mm was
252 recorded at 20 for right and left eyes respectively and was 2 times the minimum RMS of the
253 Pentacam for right eyes and 1.7 times the minimum RMS of the Pentacam for left eyes, Table
254 4.

255

256

257

258

259

260

261

262

263

264

265

266

267

268

269

270

271 Table 1: Zernike polynomial fitting RMS for both Pentacam healthy and keratoconic
 272 participants' corneal anterior surfaces.

Order n	Healthy						Keratoconic					
	Right			Left			Right			Left		
	RMS (mm)	STD (mm)	p	RMS (mm)	STD (mm)	p	RMS (mm)	STD (mm)	p	RMS (mm)	STD (mm)	p
2	0.0241	0.0071		0.0246	0.0070		0.0289	0.0126		0.0295	0.0132	
3	0.0161	0.0051	0.0000*	0.0173	0.0056	0.0000*	0.0154	0.0076	0.0000*	0.0154	0.0090	0.0000*
4	0.0039	0.0017	0.0000*	0.0042	0.0026	0.0000*	0.0073	0.0038	0.0000*	0.0073	0.0036	0.0000*
5	0.0031	0.0014	0.0000*	0.0034	0.0020	0.0000*	0.0051	0.0028	0.0000*	0.0050	0.0025	0.0000*
6	0.0021	0.0009	0.0000*	0.0023	0.0014	0.0000*	0.0034	0.0020	0.0000*	0.0036	0.0020	0.0000*
7	0.0016	0.0007	0.0000*	0.0018	0.0009	0.0000*	0.0024	0.0013	0.0000*	0.0026	0.0015	0.0000*
8	0.0012	0.0005	0.0000*	0.0013	0.0006	0.0000*	0.0016	0.0009	0.0000*	0.0018	0.0011	0.0000*
9	0.0007	0.0003	0.0000*	0.0008	0.0003	0.0000*	0.0009	0.0004	0.0000*	0.0011	0.0007	0.0000*
10	0.0004	0.0001	0.0000*	0.0004	0.0001	0.0000*	0.0005	0.0002	0.0000*	0.0006	0.0004	0.0000*
11	0.0004	0.0001	0.0000*	0.0004	0.0001	0.0000*	0.0004	0.0002	0.0001*	0.0005	0.0003	0.0089*
12	0.0003	0.0000	0.0000*	0.0003	0.0001	0.0000*	0.0004	0.0001	0.0000*	0.0004	0.0002	0.0003*
13	0.0003	0.0000	0.0005*	0.0003	0.0000	0.0023*	0.0003	0.0001	0.0364	0.0004	0.0001	0.0904
14	0.0003	0.0000	0.0000*	0.0003	0.0000	0.0051*	0.0003	0.0001	0.0344	0.0004	0.0001	0.1358
15	0.0003	0.0001	0.2883	0.0004	0.0015	0.2524	0.0003	0.0002	0.9432	0.0004	0.0003	0.8434
16	0.0004	0.0006	0.1517	0.0013	0.0112	0.1424	0.0005	0.0034	0.3280	0.0009	0.0089	0.3371
17	0.0009	0.0056	0.0978	0.0272	0.4182	0.2609	0.0024	0.0291	0.3480	0.0032	0.0398	0.4303
18	0.0126	0.1993	0.2861	0.0296	0.3099	0.9329	0.0041	0.0453	0.6251	0.0131	0.1708	0.4076
19	0.0195	0.1768	0.6371	0.0616	0.6124	0.3963	0.0317	0.3039	0.1735	0.0933	0.8995	0.2017
20	0.1221	0.8218	0.0272	0.0837	0.7085	0.6684	0.1419	1.6770	0.3275	0.0461	0.2564	0.4612

273 (*) Indicates statistical significance.

274

275

276

277 Table 2: Zernike polynomial fitting RMS for both Pentacam healthy and keratoconic
 278 participants' corneal posterior surfaces.

Order n	Healthy						Keratoconic					
	Right			Left			Right			Left		
	RMS (mm)	STD (mm)	p	RMS (mm)	STD (mm)	p	RMS (mm)	STD (mm)	p	RMS (mm)	STD (mm)	p
2	0.0409	0.0121		0.0403	0.0113		0.0467	0.0173		0.0468	0.0185	
3	0.0271	0.0083	0.0000*	0.0290	0.0095	0.0000*	0.0264	0.0100	0.0000*	0.0259	0.0107	0.0000*
4	0.0079	0.0027	0.0000*	0.0092	0.0040	0.0000*	0.0137	0.0057	0.0000*	0.0137	0.0062	0.0000*
5	0.0060	0.0025	0.0000*	0.0070	0.0036	0.0000*	0.0101	0.0042	0.0000*	0.0104	0.0047	0.0000*
6	0.0045	0.0021	0.0000*	0.0052	0.0028	0.0000*	0.0067	0.0028	0.0000*	0.0073	0.0036	0.0000*
7	0.0034	0.0016	0.0000*	0.0040	0.0021	0.0000*	0.0044	0.0022	0.0000*	0.0050	0.0025	0.0000*
8	0.0021	0.0011	0.0000*	0.0025	0.0013	0.0000*	0.0023	0.0013	0.0000*	0.0027	0.0016	0.0000*
9	0.0010	0.0004	0.0000*	0.0013	0.0008	0.0000*	0.0011	0.0007	0.0000*	0.0014	0.0009	0.0000*
10	0.0003	0.0000	0.0000*	0.0003	0.0000	0.0000*	0.0003	0.0000	0.0000*	0.0003	0.0000	0.0000*
11	0.0003	0.0000	0.1854	0.0003	0.0000	0.1287	0.0003	0.0000	0.1412	0.0003	0.0000	0.1347
12	0.0003	0.0000	0.1302	0.0003	0.0000	0.1189	0.0003	0.0000	0.1168	0.0003	0.0000	0.1028
13	0.0003	0.0000	0.0945	0.0003	0.0000	0.1326	0.0003	0.0000	0.0806	0.0003	0.0000	0.2370
14	0.0003	0.0000	0.1915	0.0003	0.0000	0.2725	0.0003	0.0000	0.3678	0.0003	0.0000	0.4210
15	0.0003	0.0000	0.2073	0.0003	0.0004	0.1627	0.0003	0.0001	0.3322	0.0003	0.0004	0.3246
16	0.0003	0.0005	0.1229	0.0006	0.0036	0.1142	0.0004	0.0012	0.3042	0.0005	0.0034	0.3696
17	0.0007	0.0040	0.1296	0.0033	0.0292	0.0962	0.0013	0.0129	0.3043	0.0018	0.0208	0.3933
18	0.0088	0.1036	0.1560	0.0131	0.1229	0.1618	0.0083	0.1082	0.3281	0.0053	0.0671	0.4680
19	0.0304	0.3227	0.2482	0.0313	0.2292	0.2022	0.0183	0.1476	0.4048	0.0092	0.0803	0.5785
20	0.0543	0.3517	0.3634	0.1686	1.5001	0.1003	0.0685	0.6656	0.2648	0.0645	0.4053	0.0517

279 (*) Indicates statistical significance.

280

281

282 Table 3: Zernike polynomial fitting RMS for Medmont Placido disc healthy participants.

Order n	Healthy					
	Right			Left		
	RMS (mm)	STD (mm)	p	RMS (mm)	STD (mm)	p
2	0.0773	0.0226		0.0759	0.0226	
3	0.0700	0.0208	0.0000*	0.0695	0.0206	0.0000*
4	0.0238	0.0091	0.0000*	0.0233	0.0090	0.0000*
5	0.0209	0.0080	0.0000*	0.0208	0.0079	0.0000*
6	0.0138	0.0064	0.0000*	0.0138	0.0060	0.0000*
7	0.0127	0.0057	0.0123*	0.0127	0.0054	0.0096*
8	0.0115	0.0051	0.0017*	0.0116	0.0050	0.0017*
9	0.0107	0.0045	0.0294*	0.0108	0.0046	0.0393*
10	0.0099	0.0041	0.0182*	0.0100	0.0044	0.0120*
11	0.0093	0.0039	0.0492*	0.0093	0.0041	0.0605
12	0.0086	0.0037	0.0079*	0.0086	0.0039	0.0130*
13	0.0080	0.0034	0.0759	0.0080	0.0035	0.0599
14	0.0074	0.0032	0.0232*	0.0074	0.0032	0.0198*
15	0.0070	0.0030	0.0895	0.0069	0.0029	0.0525
16	0.0064	0.0028	0.0511	0.0063	0.0027	0.0275*
17	0.0060	0.0026	0.1002	0.0059	0.0025	0.0804
18	0.0055	0.0024	0.1557	0.0055	0.0023	0.0635
19	0.0051	0.0022	0.2847	0.0051	0.0021	0.1050
20	0.0047	0.0021	0.3942	0.0046	0.0019	0.1290

(*) Indicates statistical significance.

283

284

285

286

Table 4: Zernike polynomial fitting RMS for ESP healthy participants

Order n	Healthy					
	Right			Left		
	RMS (mm)	STD (mm)	p	RMS (mm)	STD (mm)	p
2	0.0131	0.0028		0.0129	0.0029	
3	0.0111	0.0027	0.0000*	0.0113	0.0029	0.0000*
4	0.0046	0.0017	0.0000*	0.0049	0.0021	0.0000*
5	0.0037	0.0014	0.0000*	0.0040	0.0018	0.0001*
6	0.0029	0.0012	0.0000*	0.0031	0.0015	0.0000*
7	0.0025	0.0011	0.0048*	0.0027	0.0014	0.0176*
8	0.0022	0.0011	0.0098*	0.0023	0.0012	0.0245*
9	0.0019	0.0010	0.0390*	0.0020	0.0011	0.0412*
10	0.0017	0.0009	0.0653	0.0018	0.0010	0.0645
11	0.0015	0.0008	0.0834	0.0016	0.0009	0.0631
12	0.0013	0.0007	0.0996	0.0014	0.0007	0.0676
13	0.0011	0.0007	0.0761	0.0012	0.0007	0.1177
14	0.0010	0.0006	0.1056	0.0011	0.0006	0.0912
15	0.0009	0.0006	0.1341	0.0010	0.0006	0.1049
16	0.0008	0.0005	0.1591	0.0009	0.0005	0.1198
17	0.0007	0.0005	0.1928	0.0008	0.0004	0.1363
18	0.0007	0.0004	0.1636	0.0007	0.0004	0.1378
19	0.0006	0.0004	0.2333	0.0006	0.0004	0.1339
20	0.0005	0.0003	0.2020	0.0006	0.0003	0.1258

287

(*) Indicates statistical significance.

288

289

290

291 **Discussion**

292 Although tomographer, topographers and surface profilers are widely accepted in scientific
293 research, some of them do not offer a direct measure of topography. Numerous studies
294 published data collected from Pentacam and several compared its performance to that of other
295 topographers and reported high correlation ^{3, 20-23}. It is also important to acknowledge the
296 studies suggested that repeatability of Scheimpflug devices can be lower for the posterior
297 corneal surface than for the anterior corneal surface ^{24, 25} however, measurements taken with
298 the Pentacam are reported to be repeatable and reproducible when they are obtained with the
299 high-resolution settings and analysed with caution ²⁶.

300 Placido-disk topography systems have their limitations too. Placido-disc based systems,
301 unlike Pentacam HR, cannot provide measurements for the posterior surface of the cornea.
302 Posterior elevation data were reported to have a significant effect on overall corneal
303 astigmatism magnitude, astigmatism axis ^{25, 27}, optical axis ¹⁸ and keratoconus cone location
304 ²⁸. In addition, they cannot measure the corneal central zone within the first mire ring, and as
305 a result, this region has to be interpolated using a relatively narrow ($\cong 60\%$) corneal surface
306 coverage ^{29, 30}. They use images obtained from light reflected off the tear film, thus the
307 inconsistent quality of corneal tear film becomes an essential limitation. Moreover, Placido-
308 disk systems data are less accurate when mapping irregular surfaces due to their methodology
309 hypothesis of significant smoothness in the radial direction ³¹.

310 Like the other two devices, the ESP has some limitations. It is not possible to use eye profile
311 data without considering a method of removing the edge-effect. The artefacts around the
312 edges are not naturally present features but appear on the measured surface as a result of
313 the instrument limitation, the measurement protocol and the technological limits ¹².

314

315 The difference between a corneal measured feature and its true value is a measurement error
316 that could be either random, systematic ³² or a combination of both along with other factors.

317 Random errors naturally occur during any measurement because of disturbances such as
318 environmental conditions or electronic noise. The positive element is that random errors have
319 a Gaussian normal distribution, therefore, statistical methods can be effectively used to
320 analyse the measured data and determine the significance of any change in the measured
321 feature regardless of the associated random errors. Systematic errors usually occur as a result
322 of using a miscalibrated instrument or because of the incorrect use by the operator ³³. Although
323 these errors are important to consider, they are not the only artefacts in the corneal structure
324 measurement process. There is something else embedded within the instruments' software
325 packages called DSP. Among many other aspects, DSP involves detection, estimation,
326 coding, transmission, enhancement, analysis, representation, recording, reconstruction,
327 transformation and interpretation of digital signals ³⁴. With no access to the tomographers and
328 topographers' built-in pieces of DSP within their software, reverse engineering is one of the
329 best methods for researchers to investigate unseen DSP components. DSP within the output
330 researchers get may affect their interpretation or their understanding of the numerical values
331 produced by eye reconstruction software-driven instruments.

332

333 The technique used in this study can be considered a reverse engineering fitting method. The
334 results showed that the posterior corneal surface measured by Pentacam fits perfectly to order
335 10 Zernike polynomials with a very small RMS (3×10^{-4}) and zero standard deviation. This
336 finding indicates the possibility of the Pentacam posterior corneal surface being fitted to order
337 10 Zernike polynomials during the DSP stage. This conclusion is supported by the fact that
338 fitting the posterior surface to orders up to 15 did not record significant reductions in RMS
339 compared to order 10. It is also supported by the fact that both healthy and keratoconic
340 participants data showed the exact trend with no noticeable difference. This indicates that this
341 fitting is potentially a built-in DSP sequence within the Pentacam software.

342 On the other hand, the anterior surface of the Pentacam fitted very well to order 12 Zernike
343 polynomials in both healthy and keratoconic participants. While healthy eyes still fit well up to

344 order 14, the significance test showed that keratoconic eyes are not recoding improvement in
345 RMS values after order 12. With a standard deviation of nearly zero, there is a strong
346 possibility that a fit of order 12 Zernike polynomials was applied to anterior eye surfaces within
347 the Pentacam DSP stage. The closest study to the current one was presented by Smolek, in
348 2005, on TMS-1 (Tomey, Inc, AZ, US) corneal topography maps where he concluded that 4th
349 order Zernike polynomial reconstruction was reliable for modelling the normal cornea only, but
350 significantly higher orders are needed for reconstructing abnormal corneal surfaces ³⁵.
351 However, the current study findings do not endorse 4th order Zernike polynomial reconstruction
352 for Pentacam HR tomographer, Medmont E300 Placido-disc and ESP data. The reverse
353 engineering technique used here showed unique compatibility between the Pentacam
354 elevation data and Zernike polynomials. In addition, the RMS started to rise again after certain
355 order as an indication of an overfitting issue which is known to be associated with polynomial
356 fitting. None of the other two machines shown any rise in RMS as a result of increasing the
357 fitting order.

358 A possible limitation in this study is not splitting the data according to age groups or ethnic
359 background and not grouping keratoconic groups according to the severity of the disease. As
360 the focus of this study is the DSP within the pieces of the instrument's software, the
361 participants' data were analysed according to the instrument not according to the age groups
362 or the ethnic background. The only exception was analysing the keratoconic Pentacam data
363 separately from the healthy ones to investigate the response of distorted eyes to the Zernike
364 polynomial fitting process. Limitations of not testing keratoconic eyes or even animal eyes will
365 be addressed soon in a future study. Additionally, Zernike polynomials are not the only type
366 of polynomials that could be used to fit corneal surfaces. Tchebichef ³⁶, Krawtchouk ³⁷, Charlier
367 ³⁸, and Meixner polynomials ³⁹ could be used too, however, Zernike polynomials are broadly
368 deemed to be the mathematical base of ocular aberrations ⁴⁰.

369 The results suggest using order 10 Zernike polynomial to fit Pentacam posterior corneal
370 surface and order 12 Zernike polynomial to fit Pentacam anterior surface is an ideal option to

371 analysts who are interested in wavefront analyses, high order aberrations, light raytracing, and
372 other applications that require parametric continuous surfaces to operate. Fitting Medmont
373 E300 Placido-disc and ESP to Zernike polynomials is not recommended because of the
374 relatively high RMS associated with this fit, however, if necessary Medmont E300 Placido-
375 disc's topography and ESP's corneal profile could be fitted to Zernike polynomial order 16 and
376 9 to respectively with a consciousness of the possible effect of the fitting error.

377

378

379 **Financial Disclosure**

380 No additional external funding was received for this study.

381

382 **References**

383 1. Finis D, Ralla B, Karbe M, Borrelli M, Schrader S, Geerling G. Comparison of Two
384 Different Scheimpflug Devices in the Detection of Keratoconus, Regular
385 Astigmatism, and Healthy Corneas. *Journal of Ophthalmology* 2015 04/14

386 01/21/received

387 04/01/accepted;2015:315281. doi: 10.1155/2015/315281. PubMed PMID:
388 PMC4411433.

389 2. Al-Ageel S, Al-Muammar AM. Comparison of central corneal thickness
390 measurements by Pentacam, noncontact specular microscope, and ultrasound
391 pachymetry in normal and post-LASIK eyes. *Saudi journal of ophthalmology : official
392 journal of the Saudi Ophthalmological Society* 2009 Oct;23(3-4):181-7. doi:
393 10.1016/j.sjopt.2009.10.002. PubMed PMID: 23960858; PubMed Central PMCID:
394 PMCPMC3729515. eng.

395 3. Otchere H, Sorbara L. Repeatability of topographic corneal thickness in
396 keratoconus comparing Visante™ OCT and Oculus Pentacam HR® topographer.
397 *Contact Lens and Anterior Eye* 2017 2017/08/01;40(4):217-223. doi:
398 <http://dx.doi.org/10.1016/j.clae.2017.05.002>.

399 4. Salouti R, Nowroozzadeh MH, Zamani M, Ghoreyshi M, Salouti R. Comparison of
400 anterior chamber depth measurements using Galilei, HR Pentacam, and Orbscan II.
401 *Optometry* 2010 Jan;81(1):35-9. doi: 10.1016/j.optm.2009.04.100. PubMed PMID:
402 20004876.

403 5. Moazzam F, Bednarek MD. Intellectual Property Protection for Medical Devices.
404 In: Becker KM, Whyte JJ, editors. *Clinical Evaluation of Medical Devices: Principles
405 and Case Studies*. Totowa, NJ: Humana Press; 2006. p. 117-139.

- 406 6. Zuckerman D, Brown P, Das A. Lack of Publicly Available Scientific Evidence on
407 the Safety and Effectiveness of Implanted Medical Devices. *JAMA Internal Medicine*
408 2014;174(11):1781-1787. doi: 10.1001/jamainternmed.2014.4193.
- 409 7. RONQUILLO JG, ZUCKERMAN DM. Software-Related Recalls of Health
410 Information Technology and Other Medical Devices: Implications for FDA Regulation
411 of Digital Health. *The Milbank Quarterly* 2017;95(3):535-553. doi:
412 <https://doi.org/10.1111/1468-0009.12278>.
- 413 8. Consejo A, Llorens-Quintana C, Radhakrishnan H, Iskander DR. Mean shape of
414 the human limbus. *J Cataract Refract Surg* 2017 2017/05/01;43(5):667-672. doi:
415 10.1016/j.jcrs.2017.02.027.
- 416 9. Abass A, Lopes BT, Eliasy A, Wu R, Jones S, Clamp J, Ambrósio R, Jr., Elsheikh
417 A. Three-dimensional non-parametric method for limbus detection. *PLOS ONE*
418 2018;13(11):e0207710. doi: 10.1371/journal.pone.0207710.
- 419 10. Consejo A, Radhakrishnan H, Iskander DR. Scleral changes with
420 accommodation. *Ophthalmic & physiological optics : the journal of the British College*
421 *of Ophthalmic Opticians* 2017 May;37(3):263-274. doi: 10.1111/opo.12377. PubMed
422 PMID: 28439975; eng.
- 423 11. Consejo A, Llorens-Quintana C, Bartuzel MM, Iskander DR, Rozema JJ.
424 Rotation asymmetry of the human sclera. *Acta Ophthalmol* 2018 Aug 26. doi:
425 10.1111/aos.13901. PubMed PMID: 30146759; eng.
- 426 12. Abass A, Lopes BT, Eliasy A, Salomao M, Wu R, White L, Jones S, Clamp J,
427 Ambrósio R, Jr., Elsheikh A. Artefact-free topography based scleral-asymmetry.
428 *PLOS ONE* 2019;14(7):e0219789. doi: 10.1371/journal.pone.0219789.
- 429 13. Abass A, Clamp J, Bao F, Ambrosio R, Jr., Elsheikh A. Non-Orthogonal Corneal
430 Astigmatism among Normal and Keratoconic Brazilian and Chinese populations.
431 *Curr Eye Res* 2018 Feb 2:1-8. doi: 10.1080/02713683.2018.1433858. PubMed
432 PMID: 29393696; eng.
- 433 14. Abass A, Stuart S, Lopes BT, Zhou D, Geraghty B, Wu R, Jones S, Flux I,
434 Stortelder R, Snepvangers A, Leca R, Elsheikh A. Simulated optical performance of
435 soft contact lenses on the eye. *PLOS ONE* 2019;14(5):e0216484. doi:
436 10.1371/journal.pone.0216484.
- 437 15. Abass A, Vinciguerra R, Lopes BT, Bao F, Vinciguerra P, Ambrósio R, Elsheikh
438 A. Positions of Ocular Geometrical and Visual Axes in Brazilian, Chinese and Italian
439 Populations. *Current Eye Research* 2018 2018/11/02;43(11):1404-1414. doi:
440 10.1080/02713683.2018.1500609.
- 441 16. Consejo A, Wu R, Abass A. Anterior Scleral Regional Variation between Asian
442 and Caucasian Populations. *J Clin Med* 2020 Oct 25;9(11). doi:
443 10.3390/jcm9113419. PubMed PMID: 33113864; PubMed Central PMCID:
444 PMCPMC7692638. eng.
- 445 17. Moore J, Lopes BT, Eliasy A, Geraghty B, Wu R, White L, Elsheikh A, Abass A.
446 Simulation of the Effect of Material Properties on Soft Contact Lens On-Eye Power.
447 *Bioengineering (Basel, Switzerland)* 2019 Oct 9;6(4). doi:
448 10.3390/bioengineering6040094. PubMed PMID: 31600967; eng.
- 449 18. Lopes BT, Eliasy A, Elhalwagy M, Vinciguerra R, Bao F, Vinciguerra P, Ambrósio
450 R, Elsheikh A, Abass A. Determination of Optic Axes by Corneal Topography among
451 Italian, Brazilian, and Chinese Populations. *Photonics* 2021;8(2):61. PubMed PMID:
452 doi:10.3390/photonics8020061.
- 453 19. Everitt BS, Skrondal A. *The Cambridge Dictionary of Statistics*. 4 ed. Cambridge,
454 UK: Cambridge University Press; 2010.

- 455 20. Dehnavi Z, Mirzajani A, Jafarzadehpur E, Khabazkhoob M, Jabbarvand M, Yekta
456 A. Comparison of the corneal power measurements with the TMS4-topographer,
457 pentacam HR, IOL master, and javal keratometer [Article]. Middle East African
458 Journal of Ophthalmology 2015 04 / 01 /;22(2):233-237. doi: 10.4103/0974-
459 9233.151884. PubMed PMID: edselc.2-52.0-84926679928; English.
- 460 21. Read SA, Collins MJ, Iskander DR, Davis BA. Corneal topography with
461 Scheimpflug imaging and videokeratography: Comparative study of normal eyes.
462 Journal of Cataract & Refractive Surgery 2009 2009/06/01/;35(6):1072-1081. doi:
463 <http://dx.doi.org/10.1016/j.jcrs.2009.01.020>.
- 464 22. Tajbakhsh Z, Salouti R, Nowroozzadeh MH, Zamani M, Aghazadeh-Amiri M,
465 Tabatabaee S. Comparison of keratometry measurements using the Pentacam HR,
466 the Orbscan Ilz, and the TMS-4 topographer [Article]. Ophthalmic and Physiological
467 Optics 2012 11 / 01 /;32(6):539-546. doi: 10.1111/j.1475-1313.2012.00942.x.
468 PubMed PMID: edselc.2-52.0-84867410213; English.
- 469 23. de Jong T, Sheehan MT, Dubbelman M, Koopmans SA, Jansonius NM. Shape of
470 the anterior cornea: Comparison of height data from 4 corneal topographers. Journal
471 of Cataract & Refractive Surgery 2013 2013/10/01/;39(10):1570-1580. doi:
472 <http://dx.doi.org/10.1016/j.jcrs.2013.04.032>.
- 473 24. Koch DD, Jenkins RB, Weikert MP, Yeu E, Wang L. Correcting astigmatism with
474 toric intraocular lenses: effect of posterior corneal astigmatism. Journal of cataract
475 and refractive surgery 2013 Dec;39(12):1803-9. doi: 10.1016/j.jcrs.2013.06.027.
476 PubMed PMID: 24169231; eng.
- 477 25. Preussner PR, Hoffmann P, Wahl J. Impact of Posterior Corneal Surface on
478 Toric Intraocular Lens (IOL) Calculation. Curr Eye Res 2015;40(8):809-814. doi:
479 10.3109/02713683.2014.959708. PubMed PMID: 25259550; eng.
- 480 26. McAlinden C, Khadka J, Pesudovs K. A Comprehensive Evaluation of the
481 Precision (Repeatability and Reproducibility) of the Oculus Pentacam HR.
482 Investigative ophthalmology & visual science 2011;52(10):7731-7737. doi:
483 10.1167/iovs.10-7093.
- 484 27. Zhang B, Ma J-X, Liu D-Y, Guo C-R, Du Y-H, Guo X-J, Cui Y-X. Effects of
485 posterior corneal astigmatism on the accuracy of AcrySof toric intraocular lens
486 astigmatism correction. International Journal of Ophthalmology 2016 09/18
487 05/30/received
488 11/16/accepted;9(9):1276-1282. doi: 10.18240/ijo.2016.09.07. PubMed PMID:
489 PMC5028661.
- 490 28. Eliasy A, Abass A, Lopes BT, Vinciguerra R, Zhang H, Vinciguerra P, Ambrósio
491 R, Roberts CJ, Elsheikh A. Characterization of cone size and centre in keratoconic
492 corneas. Journal of The Royal Society Interface 2020;17(169):20200271. doi:
493 doi:10.1098/rsif.2020.0271.
- 494 29. Belin MW, Khachikian SS. An introduction to understanding elevation-based
495 topography: how elevation data are displayed - a review. Clin Experiment
496 Ophthalmol 2009 Jan;37(1):14-29. doi: 10.1111/j.1442-9071.2008.01821.x. PubMed
497 PMID: 19016811.
- 498 30. Martin R. Cornea and anterior eye assessment with placido-disc keratoscopy, slit
499 scanning evaluation topography and scheimpflug imaging tomography. Indian journal
500 of ophthalmology 2018;66(3):360-366. doi: 10.4103/ijo.IJO_850_17. PubMed PMID:
501 29480244; eng.
- 502 31. Wang L, Ang R, Yildirim R. Corneal Topography and LASIK Applications. LASIK
503 (Laser in Situ Keratomileusis). Refractive Surgery: CRC Press; 2002. p. 111-138.

- 504 32. Taylor JR, Taylor SLLJR. Introduction To Error Analysis: The Study of
505 Uncertainties in Physical Measurements. University Science Books; 1997.
506 33. Bland JM, Altman DG. Statistics Notes: Measurement error. *BMJ*
507 1996;313(7059):744. doi: 10.1136/bmj.313.7059.744.
508 34. Nair BS. Digital electronics and logic design. PHI Learning Pvt. Ltd. p. 289. New
509 Delhi: Prentice-Hall of India; 2002. English.
510 35. Smolek MK, Klyce SD. Goodness-of-prediction of Zernike polynomial fitting to
511 corneal surfaces. *Journal of cataract and refractive surgery* 2005 Dec;31(12):2350-5.
512 doi: 10.1016/j.jcrs.2005.05.025. PubMed PMID: 16473230.
513 36. Mukundan R. Some computational aspects of discrete orthonormal moments.
514 *IEEE Transactions on Image Processing* 2004;13(8):1055-1059. doi:
515 10.1109/TIP.2004.828430.
516 37. AL-Utaibi KA, Abdulhussain SH, Mahmmod BM, Naser MA, Alsabab M, Sait SM.
517 Reliable Recurrence Algorithm for High-Order Krawtchouk Polynomials. *Entropy*
518 2021;23(9):1162. PubMed PMID: doi:10.3390/e23091162.
519 38. Abdul-Hadi AM, Abdulhussain SH, Mahmmod BM. On the computational aspects
520 of Charlier polynomials. *Cogent Engineering* 2020 2020/01/01;7(1):1763553. doi:
521 10.1080/23311916.2020.1763553.
522 39. Abdulhussain SH, Mahmmod BM. Fast and efficient recursive algorithm of
523 Meixner polynomials. *Journal of Real-Time Image Processing* 2021 2021/04/26. doi:
524 10.1007/s11554-021-01093-z.
525 40. Cerviño A, Hosking SL, Montes-Mico R, Bates K. Clinical Ocular Wavefront
526 Analyzers. *Journal of Refractive Surgery* 2007;23(6):603-616. doi: doi:10.3928/1081-
527 597X-20070601-12.

528

529

530

531

532

533

534

535

536

537

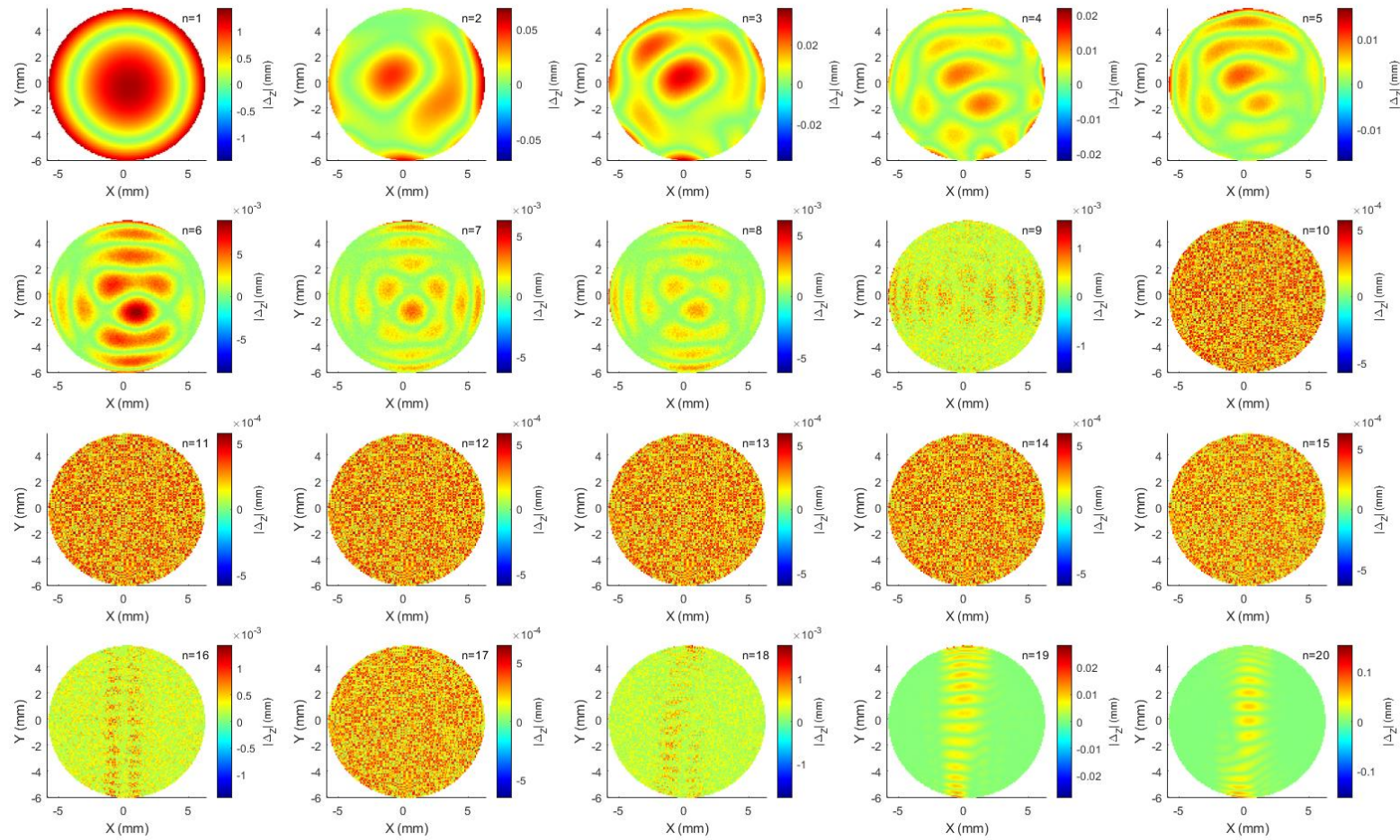
538

539

540

541

542

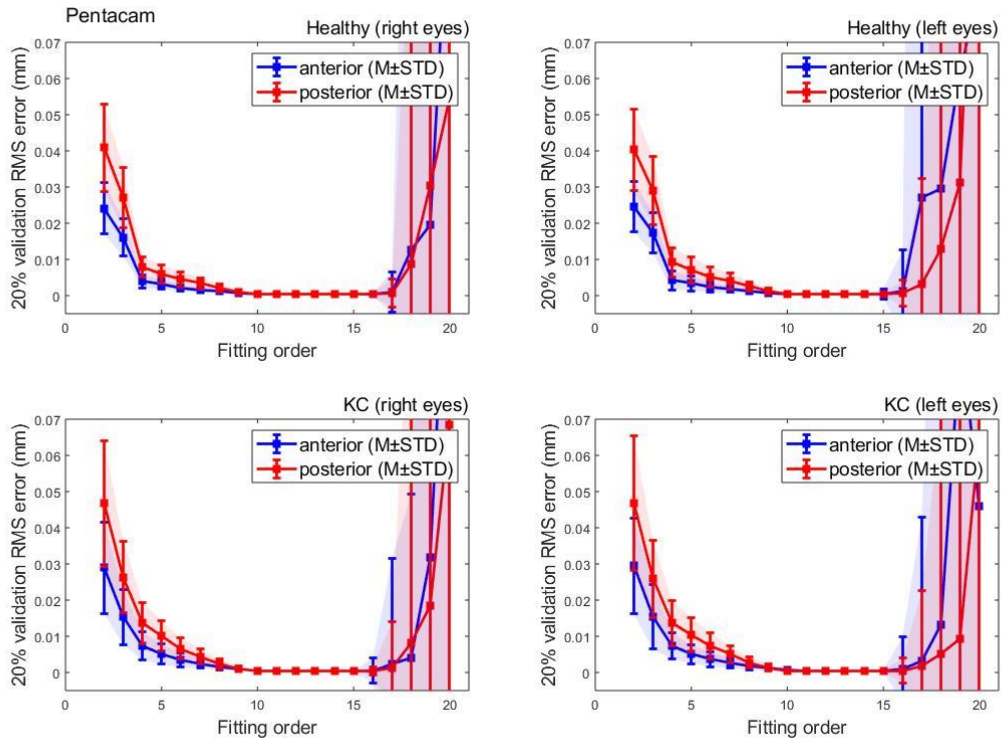


543

544 Figure 1: Zernike polynomial absolute fitting error $\Delta_z=|Z_{fit}-Z_{surf}|$ for the anterior corneal surface of 27 years old keratotic female participant
545 measured by the Pentacam HR tomographer.

546

547



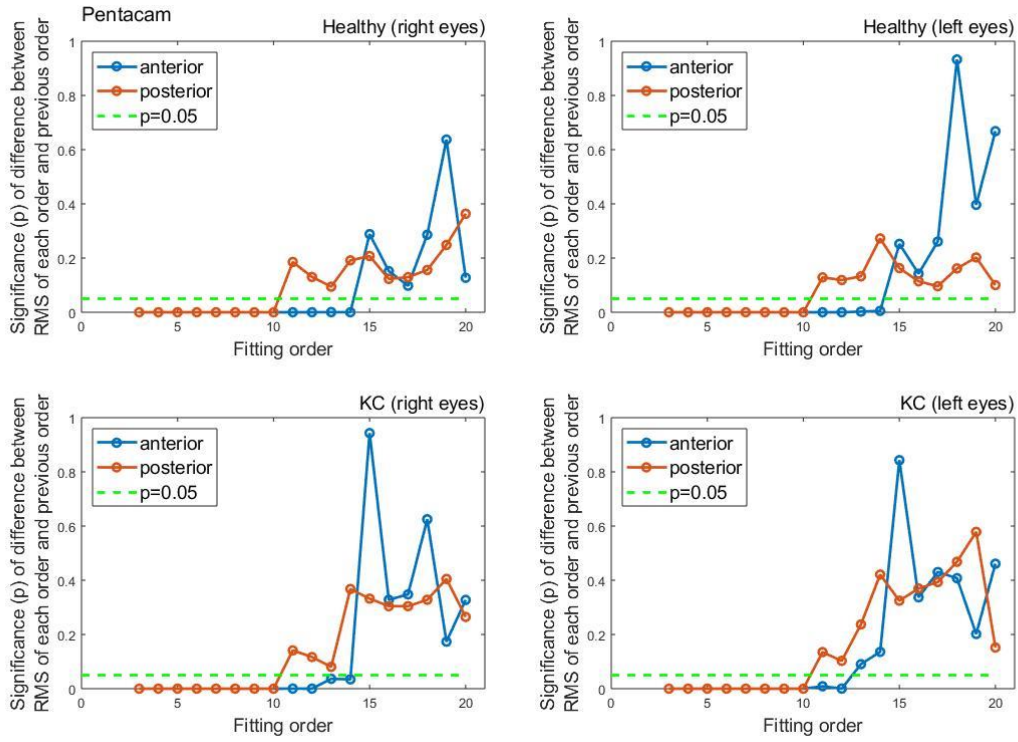
548

549 Figure 2: Pentacam HR Zernike polynomial fitting RMS error with 20% validation for healthy
550 and keratotic populations.

551

552

553

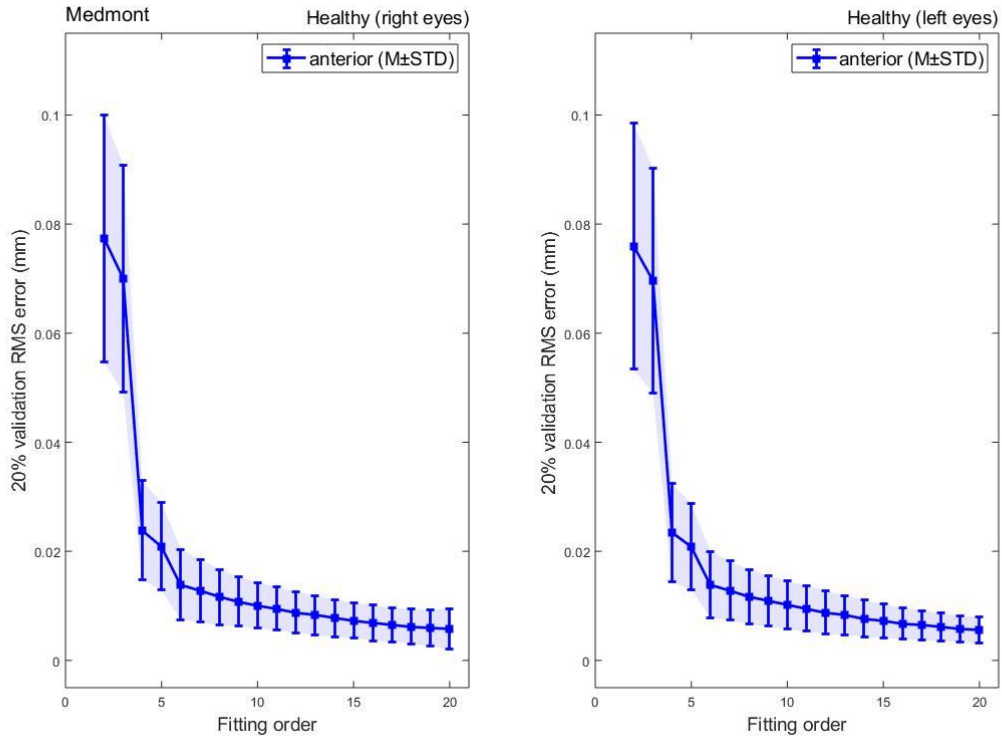


554

555 Figure 3: Significance (p) of difference between RMS of each order and previous order among
556 normal and keratoconic cases.

557

558



559

560 Figure 4: Medmont Zernike polynomial fitting RMS error with 20% validation for a healthy
561 population.

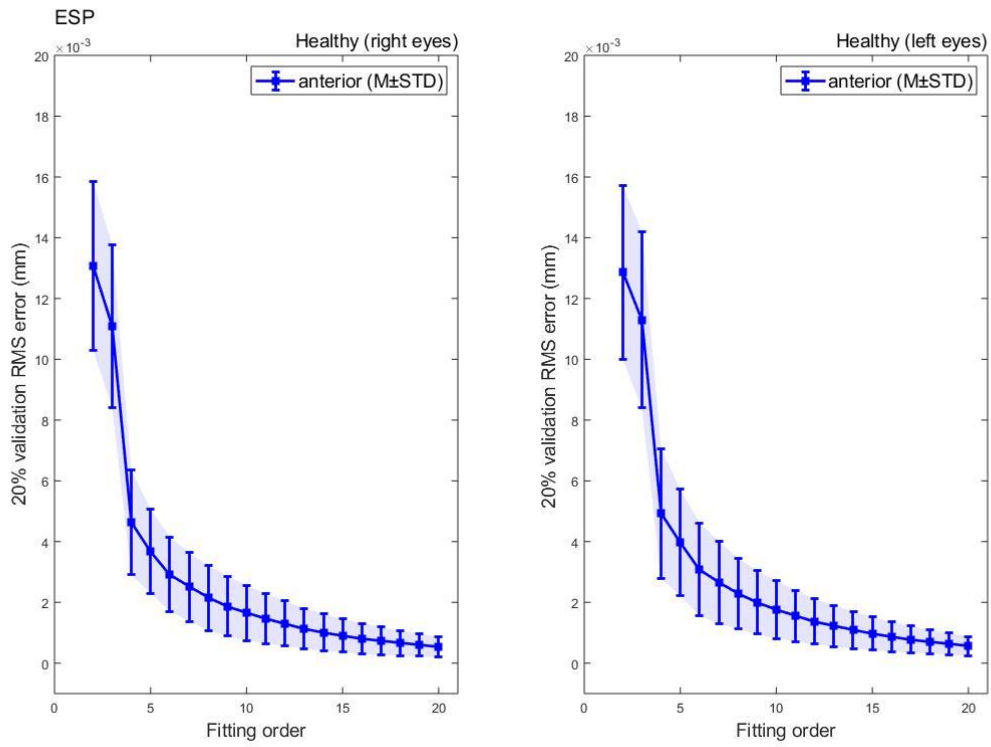


Figure 5: ESP Zernike polynomial fitting RMS error with 20% validation for a healthy population.